frontiers | Frontiers in Plant Science

TYPE Original Research
PUBLISHED 27 October 2025
DOI 10.3389/fpls.2025.1669365

Check for updates

OPEN ACCESS

EDITED BY
Weichao Wang,
Shihezi University, China

REVIEWED BY
Bai-Xiong Chen,
Zhuhai Campus of Zunyi Medical University, China
Artur Pinski,
University of Silesia in Katowice, Poland

*CORRESPONDENCE
Changying Liu
lcyswu@163.com

RECEIVED 19 July 2025
ACCEPTED 09 October 2025
PUBLISHED 27 October 2025

CITATION
Liu C, Wang J, Qiu Q, Xu D, Wu X, Yin J, Zheng X, Tan M, Wan Y, Sun W and Xiang D (2025) Physiological, transcriptomic, and genomic analysis unravels the response of Tatary buckwheat root to high ammonium stress. *Front. Plant Sci.* 16:1669365. doi: 10.3389/fpls.2025.1669365

COPYRIGHT
© 2025 Liu, Wang, Qiu, Xu, Wu, Yin, Zheng, Tan, Wan, Sun and Xiang. This is an open-access article distributed under the terms of the Creative Commons Attribution License (CC BY). The use, distribution or reproduction in other forums is permitted, provided the original author(s) and the copyright owner(s) are credited and that the original publication in this journal is cited, in accordance with accepted academic practice. No use, distribution or reproduction is permitted which does not comply with these terms.

Physiological, transcriptomic, and genomic analysis unravels the response of Tatary buckwheat root to high ammonium stress

Changying Liu[1,2]*, Jiting Wang[1,2], Qingcheng Qiu[1,2], Daiying Xu[1,2], Xi Wu[1,2], Junjie Yin[1,2], Xiaoqin Zheng[1,2], Maoling Tan[1,2], Yan Wan[1,2], Wenjun Sun[1,2] and Dabing Xiang[1,2]

[1]Key Laboratory of Coarse Cereal Processing, Ministry of Agriculture and Rural Affairs, Sichuan Engineering and Technology Research Center of Coarse Cereal Industrialization, Chengdu University, Chengdu, Sichuan, China, [2]School of Food and Biological Engineering, Chengdu University, Chengdu, Sichuan, China

Toxicity caused by high ammonium severely affects plant growth and crop production, it is urgent to breed high NH_4^+-tolerant and high-yield plants. However, the molecular mechanisms on the response and tolerance of plant to high NH_4^+ remain poorly understood. In this study, four different genotypes of Tartary buckwheat (*Fagopyrum tataricum* Garetn.) were used to investigate the molecular mechanism on high NH_4^+ response by integrating physiological, transcriptome, and genome analysis. The root and shoot growth of Tartary buckwheat (TB) seedlings were significantly inhibited by 50 and 100 mmol/L NH_4^+ treatments. High NH_4^+ inhibits root growth by affecting activities of antioxidant enzymes, thereby suppressing plant growth. In total 426 high NH_4^+-responsive common differentially expressed genes (DEGs) were identified in TB. Most of DEGs involved in antioxidant enzyme system, hormone signaling, and N transport and assimilation were down-regulated by high NH_4^+. Co-expression analysis suggested the possible hub genes in regulating high NH_4^+ response, such as *FtNRT1.14*, *FtMYB61/52*, *FtbZIP6/34*, *FtNAC72/73*, and *FtLTP14*. 19 small secreted peptides (SSPs) encoding genes were respond to high NH_4^+, including *FtCLE7* and *FtCEP3*. The up-regulation of *FtCLE7* expression and down-regulation of *FtCEP3* expression may help plants to optimize root perception and response to high NH_4^+. Additionally, 443 genotype-specific high NH_4^+-responsive DEGs with sequence variation were identified by integrating transcriptome and genome re-sequencing data. The *TFs* such as *MYB*, *MADS*, and *LBD* genes and the *RLKs* such as *FtBAM1/3* may help TB to adapt to high NH_4^+. This work provides useful information for investigating the mechanisms on TB respond to high NH_4^+, and the candidate genes for breeding TB with high NH_4^+ tolerance were suggested.

KEYWORDS

genome re-sequencing, high NH_4^+, root, Tartary buckwheat, transcriptome

1 Introduction

Nitrogen (N) is important for maintaining plant growth, development, and metabolism, which is also the major component of nucleic acids, proteins, chlorophyll, and many metabolites (Zhu et al., 2022b). N is taken up by plant roots in inorganic form such as nitrate, ammonium, and organic form including urea, amino acids, and peptides (Liu and von Wirén, 2017). Ammonium, nitrate, urea, and anhydrous ammonia were typically used as N fertilizers for improving crop growth and yield (Bittsánszky et al., 2015). Ammonium-related fertilizers are widely used due to ammonium is preferred N source for plants (Li et al., 2024). In practical crop production, urea is the worldwide leading N fertilizer, which is converted to ammonium by urease enzymes of soil microorganisms and then was absorbed by crops (Bittsánszky et al., 2015). However, ammonium-based fertilizers are excessively applied in intensive farming, which cause serious harm ammonium toxicity to plant growth and many environmental problems (Sun et al., 2022). The phenomenon of ammonium toxicity on plants was firstly found by Charles Darwin in 1882, which has now become a global problem (Bittsánszky et al., 2015). The main symptoms caused by ammonium toxicity include leaf chlorosis, rhizosphere acidification, decreases in root/shoot growth, cation uptake, photosynthesis, and yield, increases in photorespiration and oxidative stress, as well as osmotic and hormonal imbalance (Esteban et al., 2016). Therefore, it is urgent to lower the application of ammonium fertilizer and improve the tolerance and amelioration of crops against ammonium toxicity. Improving high ammonium tolerance and N use efficiency of crop through genetic engineering will be a promising approach for ensuring crop yield. However, the molecular mechanisms on the response and tolerance of plant to ammonium remain poorly understood. Elucidation of the molecular mechanism on the response to high ammonium could facilitate the improvement of high ammonium-tolerant and high-yield crops (Smoczynska et al., 2022).

In plants, ammonium was taken up by the roots via non-selective cation channels, potassium channels, aquaporins or ammonium transporters (AMTs) (Bittsánszky et al., 2015). Once ammonium enters into plant cells, it is assimilated into glutamine and glutamate via the glutamine synthetase (GS) and glutamate synthase (GOGAT) cycle. NADH-dependent glutamate dehydrogenase (GDH) synthesizes glutamate in the cytosol by using ammonium and 2-oxoglutarate (Liu and von Wirén, 2017). Besides, asparagine synthetase (ASN) and asparagine aminotransferase (ASP) can also transform ammonium into aspartate (Xu et al., 2012). Above foundational studies suggested that ammonium sensitivity of plant can be changed by manipulating AMT and N metabolism enzymes. Knockout of *AMT* genes in rice and *Arabidopsis* resulted in significant reduction in NH_4^+ uptake (Sonoda et al., 2003; Konishi and Ma, 2021). In poplar, overexpressing *GS1;2* gene increased tolerance to ammonium toxicity by maintaining carbon and N balance (Leng et al., 2024). In *Populus* × *xiaohei*, overexpression of alanine aminotransferase (*AlaAT*) gene enhances the tolerance of plants to ammonium toxicity (Yang et al., 2025). In addition, heterologous expression of a fungal *GDH* gene in rice alleviated ammonium toxicity and suppressed photorespiration (Yan et al., 2021).

Ammonium sensitivity of plants is a research hotspot, and the molecular regulatory mechanism of ammonium toxicity on plants was studied. It was found that hormone signaling is involved in high NH_4^+ response. The ethylene (ETH) precursor 1-aminocyclopropane-1-carboxylic acid (ACC) increases shoot sensitivity to NH_4^+, and ethylene-insensitive 3 (EIN3) leading to oxidative stress caused under NH_4^+ stress by inducing shoot ROS accumulation (Li et al., 2019). Abscisic acid (ABA) modulated ammonium stress response by regulating oxidative damage and NH_4^+ accumulation (Sun et al., 2020). Jasmonate meditated signaling also involves in regulating ammonium response by suppressing iron accumulation (Pandey et al., 2024). Some previous studies suggested that nitrate can alleviate ammonium toxicity in plants. In *Brassica napus*, nitrate alleviates ammonium toxicity of by balancing rhizosphere and intracellular pH, as well as accelerating NH_4^+ assimilation (Li et al., 2024). In *Arabidopsis*, nitrate transporter NRT1.1 and nitrate efflux channel SLAH3 form a functional unit to regulate nitrate-dependent ammonium toxicity alleviation and acidity tolerance (Zheng et al., 2015; Xiao et al., 2022). SNF1-related protein kinase 1 (SnRK1.1) participated in the nitrate-dependent ammonium toxicity alleviation by phosphorylating the C-terminal of SLAH3 (Sun et al., 2021a). Additionally, some transcription factors (TFs) are essential for the tolerance of plant to high ammonium. In *Arabidopsis*, *MYB28* and *MYB29* TFs play important roles in ammonium stress response, and mutation of both two genes lowered high ammonium tolerance (Coleto et al., 2021). *WRKY46* promotes ammonium tolerance by inhibiting ammonium efflux and repressing the expression of *NUDX9* and indole-3-acetic acid-conjugating genes (Di et al., 2021). *OsNLP3*-mediated nitrate signaling conferring rice with the ability to alleviate ammonium toxicity and to adapt to the high-ammonium condition (Yan et al., 2023). In barley (*Hordeum vulgare*), *HvMADS27* expression was significant decreased under ammonium stress condition, which regulates root architecture by modulating ABA metabolism (Smoczynska et al., 2022).

Although molecular mechanism on the response and tolerance to ammonium toxicity has been studied in model plants, very little information is available regarding non-model plants. Tartary buckwheat (*Fagopyrum tataricum* Gaertn.) is an important medicinal and edible crop with a worldwide distribution (Li et al., 2025). In this study, Tartary buckwheat (TB) was used to explore the physiological and molecular mechanisms of ammonium toxicity affecting the growth and development. In our previous studies, TB was used as a model plant to clarify the physiological mechanism of root in response to N, and the key genes involved in N uptake and utilization were revealed through genome re-sequencing and root transcriptome analysis (Liu et al., 2021a, 2021b, 2023a). However, the responsive mechanisms of TB in response to high NH_4^+ remain unclear. In TB cultivation, unreasonable application of N fertilizer, especially excessive application of ammonium-based fertilizers and urea, restricted the increase in yield of TB (Qiu et al., 2023). Therefore, the physiological mechanism of high NH_4^+ affecting the growth of four different TB varieties was analyzed in this study.

The molecular mechanisms of root respond to high NH_4^+ were analyzed by transcriptome and genome analysis. The key genes regulating high ammonium response in TB root were suggested in this paper. This study will provide the basis for disclosing the molecular mechanism of TB and other crops under high NH_4^+ condition.

2 Materials and methods

2.1 Plant materials and treatments

Four TB varieties, Xiqiao No. 2 (XQ2), Fenghuang (FH), Yunqiao No. 1 (YQ1), and Yunqiao No. 2 (YQ2), were used in this study. These four varieties showed different response to N treatment (Qiu et al., 2023; Liu et al., 2023a). The seeds were sterilized with 0.7% sodium hypochlorite for 30 min and washed by ddH_2O. And then, the seeds were placed in floating culture plates. Three days after seed germination, the seedlings with a root length of about 1.5 cm were selected and placed in Hoagland hydroponic solution containing different concentrations of NH_4^+ (1, 10, 50, and 100 mmol/L). $(NH_4)_2SO_4$ was used as N source. The pH of the nutrient solution was adjusted to 5.8 ± 0.1. The nutrient solution was refreshed every three days. After six days of NH_4^+ treatment, the TB seedlings and roots were sampled, and the roots were stored at −80°C for subsequent experiments.

2.2 Morphology analysis of seedlings growth

The surface water of TB seedlings was dried with filter paper, and each plant was separated from the junction of roots and stems with scissors. The fresh weight of roots and shoots was measured, respectively. The total length of root and shoot, as well as lateral root number were measured by WinRHIZO scanning system (Version 2007d, Regent Instrument Inc., Canada).

2.3 Biochemical assays of hydroponic seedlings' root

TB seedlings cultured in Hoagland nutrient solution containing 1 mmol/L and 100 mmol/L NH_4^+ for six days were collected. The roots were washed by ddH_2O and were cut into pieces, which were used for determining the activities of superoxide dismutase (SOD), catalase (CAT), peroxidase (POD), and ascorbate peroxidase (APX), as well as malondialdehyde (MDA) content according to manufacturer's instructions of test kits (Liu et al., 2022). All these kits were purchased from Nanjing Mofan Biotechnology Co., Ltd.

2.4 Transcriptomic analysis of TB root under high NH_4^+

Four varieties of TB seedlings cultured in nutrient solution of 1 mmol/L and 100 mmol/L NH_4^+ for six days were collected. The roots were washed with ddH_2O, and then were cut off with sterilized scissors for transcriptome analysis. Weight the appropriate amount of frozen samples for total RNA extraction using Magnetic Tissue/Cell/Blood Total RNA Kit (Tiangen Biotech Co., Ltd., Beijing, China). The concentration and purity were detected by Thermo Scientific NanoDrop 2000 (Thermo Scientific, Waltham, Massachusetts, USA), and the integrity was detected by RNA 6000 Nano kit (Agilent Technologies Inc, California, USA). Total RNA with a total amount of ≥ 1 μg was used to construct the library using the NEBNext Ultra II RNA Library Prep Kit (New England Biolabs Inc., Massachusetts, USA). After that, Agilent 2100 Bioanalyzer (Agilent Technologies Inc, California, USA) and Agilent High Sensitivity DNA Kit (Agilent Technologies Inc, California, USA) were used to detect the quality of the library. The mixed library was gradually diluted and quantified, and then was sequenced on the Illumina sequencer by using PE150 mode. The raw sequencing data was submitted to NCBI Short Read Archive database (accession number: PRJNA1111253).

The raw data of the FASTQ were filtered to remove adaptor sequences at the 3' end and the reads with an average mass fraction lower than Q20. The clean reads from each library were mapped to the reference genome of TB (Zhang et al., 2017; Liu et al., 2021a). Differentially expressed genes (DEGs) between two comparisons were analyzed using DESeq (v1.38.3) software. |log2FoldChange|>1 and significant *P*-value <0.05 was set as threshold to screen DEGs. Gene ontology (GO) enrichment analysis of DEGs was performed using topGO (v2.50.0). The DEGs were subjected to pathway analysis using KEGG database (http://www.genome.ad.jp/kegg/) (Liu et al., 2023a).

2.5 Quantitative RT-PCR verification

The SYBR Premix Ex Taq II (TaKaRa) kit was used for qRT-PCR analysis. The reaction system was as follows: 2 × TB Green Premix Ex Taq II Fast qPCR (12.5 μL), upstream primer (10 μM, 1 μL), downstream primer (10 μM, 1 μL), cDNA template (2 μL), and sterile water (8.5 μL). The reaction procedure was as follows: pre-denaturation at 95°C for 30 s, denaturation at 94°C for 5 s, annealing at 60°C for 10 s, extension at 72°C for 10 min, 40 cycles (Liu et al., 2021a). *FtActin7* was selected as the internal reference gene according to the transcriptome data, and each experiment was repeated three times. The gene expression was calculated by $2^{-\Delta\Delta Ct}$ method. The primers were showed in Supplementary Table 1.

2.6 Statistical analysis

All the data were processed by Excel 2019. IBM SPSS Statistics 25 software was used to analyze the significant differences between different samples by Duncan multi-factor and independent sample-T test. GraphPad Prism 9 and Adobe Illustrator CS6 were used for drawing pictures.

3 Results

3.1 High NH_4^+ seriously affects the growth of TB

As shown in Supplementary Figure 1, with the increase of NH_4^+ concentration, the development of hydroponic seedlings of four TB varieties was inhibited. Under high NH_4^+, the root and shoot weights of seedlings were significantly inhibited by 50 and 100 mmol/L NH_4^+ treatments (Figures 1A, B). At the same time, the hydroponic seedlings under high NH_4^+ tend to decrease the shoot length, primary root length, total root length, root surface area, and root volume, while the number of lateral roots did not change (Figures 1C-H). Therefore, it is speculated that high NH_4^+ may inhibit crop growth by affecting root development.

3.2 Biochemical analysis of hydroponics seedlings growth inhibition under high NH_4^+

Biochemical analysis of the hydroponic seedlings' roots under high NH_4^+ was conducted. Compared with NN (1 mmol/L NH_4^+) treatment, HN (100 mmol/L NH_4^+) significantly affects the MDA content and CAT, SOD, POD, and APX activities of TB seedling roots (Figures 2A-E). HN significantly increased the MDA content of seedling roots, indicating that roots were seriously damaged by high NH_4^+ (Figure 2A). The activities of CAT and SOD were inhibited, and the activities of POD and APX were increased (Figures 2B-E). Correlation analysis showed that MDA content was negatively correlated with root fresh weight, total root length, root surface area, root volume, and primary root length ($P < 0.05$) (Figure 2F). The activities of CAT and SOD were significantly positively correlated with root fresh weight, total root length, root surface area, root volume, and primary root length ($P < 0.05$) (Figure 2F).

3.3 The effect of high NH_4^+ on roots at transcriptome level

In the present study, a transcriptome profiling analysis was performed to investigate the response of TB roots to high NH_4^+. A total of 152.13 Gb of high-quality bases were obtained from 24 samples (Supplementary Table 2). The proportion of bases whose quality values reached Q20 in each sample was greater than 97.25%, and proportion of bases whose quality values reached Q30 was greater than 92.38% (Supplementary Table 2). The expression data of all the detected TB genes were showed in Supplementary Table 3. It was found that the Pearson correlation coefficient between the three replicates of each treatment was greater than 0.9, and the samples had good repeatability (Figure 3A). Through PCA analysis, it was found that the samples of YQ1, YQ2, XQ2, and FH were significantly separated between NN and HN treatments (Figure 3B). A total of 2, 008 high NH_4^+-induced DEGs were screened in FH, including 825 up-regulated and 1, 183 down-regulated genes. XQ2 had 3, 371 DEGs, including 1, 125 up-regulated genes and 2, 246 down-regulated genes. YQ1 had 2, 300 DEGs, including 820 up-regulated and 1, 480 down-regulated genes. YQ2 had 2, 489 DEGs, including 992 up-regulated and 1, 497 down-regulated genes (Figure 4A). 12 genes, including *FtNRT1.10/1.22, FtNRT2.1/2.4*, *FtNRT3.1/3.2*, *FtNIR*, *FtGDH3*, *FtWRKY41*, *FtMYB52*, *FtLBD38*, and *FtNF-YA10*, were screened to verify the accuracy of transcriptome data by qRT-PCR. The expression levels of these genes determined by qRT-PCR were consistent with the expression patterns of RNA-seq data (Supplementary Figure 2).

426 common DEGs were found in all four varieties by Venn diagram analysis (Figure 4B; Supplementary Table 4). The results of the heatmap showed these genes have different expression patterns (Figure 4C). Among them, 153 genes were specifically up-regulated by high NH_4^+, 261 genes were specifically down-regulated, and 12 genes had different high NH_4^+-responsive patterns among the four TB varieties. GO enrichment analysis of 426 common DEGs showed that they were distributed in 200 GO categories. These genes were more enriched into peroxidase activity, heme binding, protein kinase activity, DNA-binding transcription factor activity, DNA binding, regulation of transcription, DNA-templated, metabolic process, transmembrane transport, protein phosphorylation, response to oxidative, obsolete oxidation-reduction process, membrane, and integral component of membrane (Figure 4D).

3.4 Expression analysis of the common DEGs in response to high NH_4^+

17 DEGs involved in antioxidant enzyme system were found in the 426 common NH_4^+-responsive DEGs (Supplementary Table 5). Among the ten *PER* genes, the expression of nine genes was significantly inhibited by HN treatment. The expression of *FtPER5* (FtPinG0000858000.01) was significantly inhibited by HN treatment in YQ1, while it was up-regulated in YQ2, XQ2, and FH (Figure 5A). The expression of three *ASOL* and one *GRX* was significantly inhibited by HN treatment, while two *GST* and one *LEA* genes were up-regulated by HN treatment (Figure 5A).

12 genes involved in hormone biosynthesis and signaling were found (Supplementary Table 5). Four ETH pathway genes were significantly inhibited by HN treatment, while the expression of *FtACO6* (FtPinG0005322400.01) showed the opposite expression pattern (Figure 5B). The three GA signaling genes were significantly inhibited by HN treatment. The genes involved in auxin (IAA) and

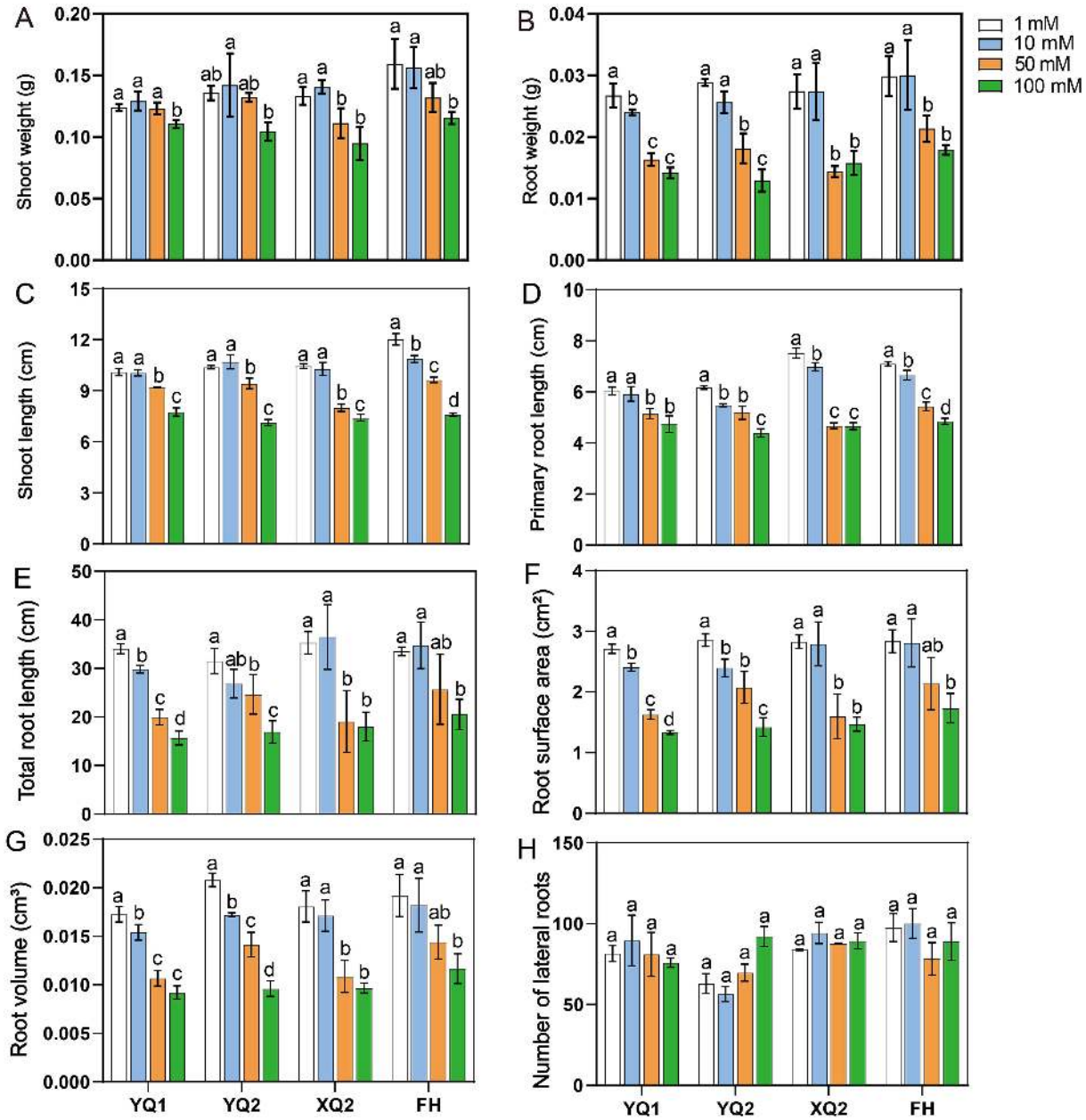

FIGURE 1
Effect of high NH_4^+ on the growth of TB hydroponics seedlings. **(A)** The weight of shoot under different concentrations of NH_4^+. **(B)** The weight of root under different concentrations of NH_4^+. **(C)** The length of shoot under different concentrations of NH_4^+. **(C, D)** The length of total root and primary root under different concentrations of NH_4^+. **(F-H)** The surface area and volume of root, as well as lateral root number of TB seedlings under high NH_4^+. Data are means ± SDs. The means were compared by Duncan's test. Different treatments of each variety marked with different lowercase letters showed significant difference ($P < 0.05$).

jasmonic acid (JA) biosynthesis were up-regulated by HN treatment. The expression patterns of genes involved in cytokinin (CTK) and ABA biosynthesis were different in the four TB varieties. Under HN treatment, the expression of *FtZOX1* (FtPinG0009420300.01) in YQ1, YQ2, and XQ2 was up-regulated, and the expression in FH was down-regulated. The expression of *FtPP2C28* (FtPinG0005550700.01) was down-regulated in YQ1, and HN treatment significantly up-regulated *FtPP2C28* expression in YQ2, XQ2, and FH (Figure 5B).

Ten DEGs involved in N transport and assimilation were found in the 426 common NH_4^+-responsive DEGs (Supplementary Table 5). Most of these genes' expression involved in N transport was significantly inhibited by HN treatment, but HN treatment significantly induced the expression of *FtNRT1.10* (FtPinG0004671100.01) (Figure 5C). The two genes involved in N assimilation, *FtNIR* and *FtGDH1*, showed different expression patterns. HN treatment significantly induced the expression of *FtGDH1* (FtPinG0008184600.01), while the expression of *FtNIR*

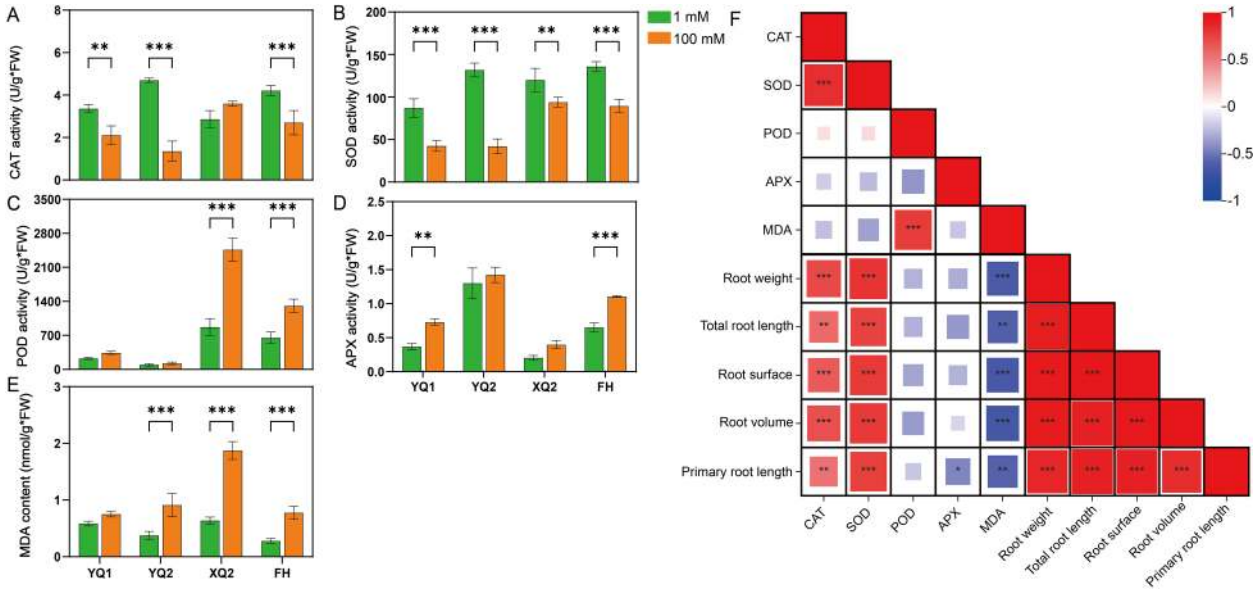

FIGURE 2
Stress analysis of TB hydroponics seedlings under high NH_4^+. **(A-E)** The activities of CAT, SOD, POD and APX, as well as MDA content in seedlings. **(F)** Correlation analysis between root morphology and enzyme activity of TB seedlings. Data are means ± SDs. The means were compared by Duncan's test. *, ** and *** indicate $P < 0.05$, $P < 0.01$ and $P < 0.001$, respectively.

(FtPinG0006174600.01) was significantly inhibited by HN (Figure 5C).

In this study, 28 TFs were identified from the 426 common DEGs (Supplementary Table 5). Within *MYB* genes, the expression of four genes (*FtMYB39/52/80* and *FtECT1*) was significantly up-regulated by HN, and two genes (*FtMYB61/83*) was inhibited by HN (Figure 6D). In NAM, ATAF1/2 and CUC2 protein (NAC) genes, there were four up-regulated genes (*FtNAC10/29/42/72*) and one down-regulated gene (*FtNAC73*). In *bZIPs*, there were two up-regulated genes (*FtbZIP1/53* and *FtHY5*) and two down-regulated genes (*FtbZIP6/34*). Within *WRKYs*, there were two up-regulated genes (*FtWRKY61/75*) and one down-regulated gene (*FtWRKY41*). Within homeobox-leucine zipper proteins (HD-ZIP) and *MADS* genes, *FtHAT22* and *FtMADS14* are up-regulated DEGs and *FtHDG1/FtAGL8* are down-regulated DEGs (Figure 5D). In addition, HN treatment significantly induced the expression of *FtLBD38* and *FtHY5*, and significantly inhibited the expression of *FtPIF3*, *FtNF-YA10*, *FtANT*, and *FtbHLH62* (Figure 5D).

In our previous study, 932 genes encoding small secreted peptides (SSPs) were reported (Liu et al., 2021b). In this paper, 19 high NH_4^+-responsive SSPs encoding genes were identified by Venn diagram analysis. Seven of these SSPs was identified as established SSPs, including one CLAVATA3/EMBRYO SURROUNDING REGION proteins (CLE), one C-terminally encoded peptide (CEP), two germin-like proteins (GLPs), two lipid transfer proteins (LTPs), and two plant defensin (PDF). Expression analysis showed that the 19 *SSP* genes performed different expression patterns in response to high NH_4^+ (Figure 5E; Supplementary Table 5). The expression of eight *SSP* genes including *FtCEP3*, *FtGLP1*, and *FtLTP14* was down-regulated by HN, while ten genes including *FtCLE7*, *FtPDF8/14*, and *FtGLP31* showed up-regulated expression pattern in all four varieties. Besides, the expression *FtLTP7* was down-regulated by HN in XQ, while HN enhanced its expression level in other three varieties (Figure 5F).

In addition, the correlations among the key high NH_4^+-responsive DEGs were analyzed, including DEGs involved in antioxidant enzyme system, hormone signaling, and N transport/assimilation, as well as TFs and SSPs encoding genes (Figure 5G). 70 of 75 these genes showed high correlation with the expression of one or more genes. Some genes, such as *FtPER60-1*, *FtASOL-1*, *FtACS7*, *FtACO1/5*, *FtNRT1.14*, *FtMYB61/52*, *FtANT*, *FtbZIP6/34*, *FtNAC72/73*, *FtLTP14*, and *FtCEP3*, may be the core genes in regulating high NH_4^+ response of TB (Figure 5G).

3.5 Identification of genotype-specific high NH_4^+-responsive DEGs

In our previous studies, the four varieties, XQ2, FH, YQ1, and YQ2, showed different sensitive to N in hydroponic and field environments, and the genotype-specific N-responsive genes was revealed (Qiu et al., 2023; Liu et al., 2023a). Therefore, these four varieties were usually used for investigating the physiological mechanism of TB in response to N in our research, including high NH_4^+. In this study, the four varieties were clustered based the fold changes of root weight, total root length, primary root length, root surface area, and root volume under 1 and 100 mmol/L NH_4^+. The four varieties showed different sensitivity to HN, and FH is less sensitive to HN stress than other three varieties (Supplementary Figure 3). For this, the difference of four varieties in response to HN at transcriptome level was investigated. 368, 1,480, 875, and 474

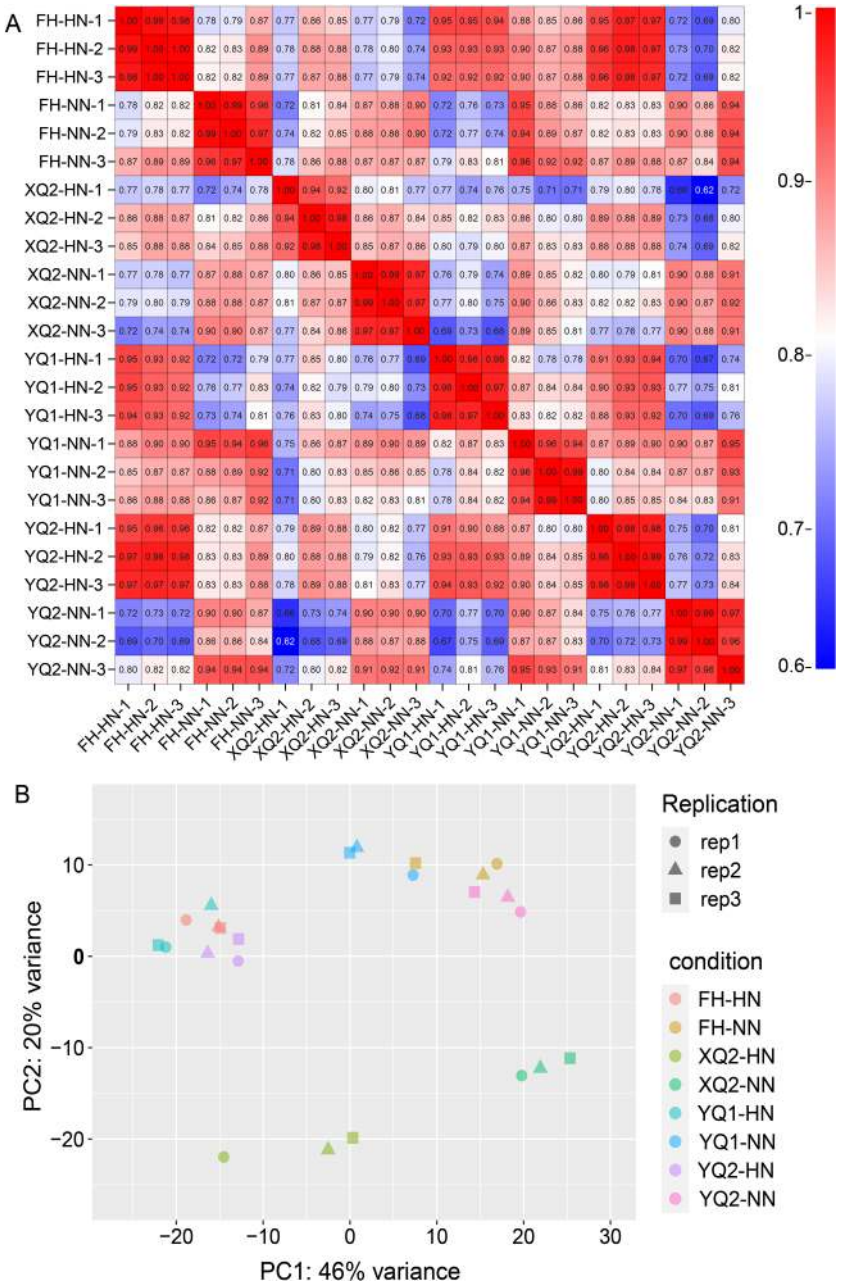

FIGURE 3
Correlation **(A)** and PCA **(B)** analysis of the RNA-seq data.

specific DEGs were found in FH, XQ2, YQ1, and YQ2, respectively (Figure 6). GO enrichment analysis showed that the 368 FH-specific DEGs were more enriched into integral component of membrane, membrane, obsolete oxidation-reduction process, metabolic process, protein phosphorylation, regulation of transcription, DNA-templated, protein kinase activity, and DNA binding. 1, 480 XQ2-specific DEGs were more enriched into integral component of membrane, nucleus, obsolete oxidation-reduction process, protein phosphorylation, metabolic process, regulation of transcription, DNA-templated, ATP binding, protein binding, and DNA binding. 875 YQ1-specific DEGs were more enriched into membrane, integral component of membrane, protein phosphorylation, regulation of transcription, DNA-templated, obsolete oxidation-reduction process, calcium ion binding, protein kinase activity, and DNA binding. 474 YQ1-specific DEGs were more enriched into membrane, integral component of membrane, nucleus, obsolete oxidation-reduction process, transmembrane transport, protein phosphorylation, regulation of transcription, DNA-templated, protein binding, ATP binding, and protein kinase activity (Figure 6).

KEGG enrichment analysis showed that the 368 FH-specific DEGs were more enriched into phenylpropanoid biosynthesis, endocytosis, plant hormone signal transduction, glycolysis, and ubiquitin mediated proteolysis. 1, 480 XQ2-specific DEGs were

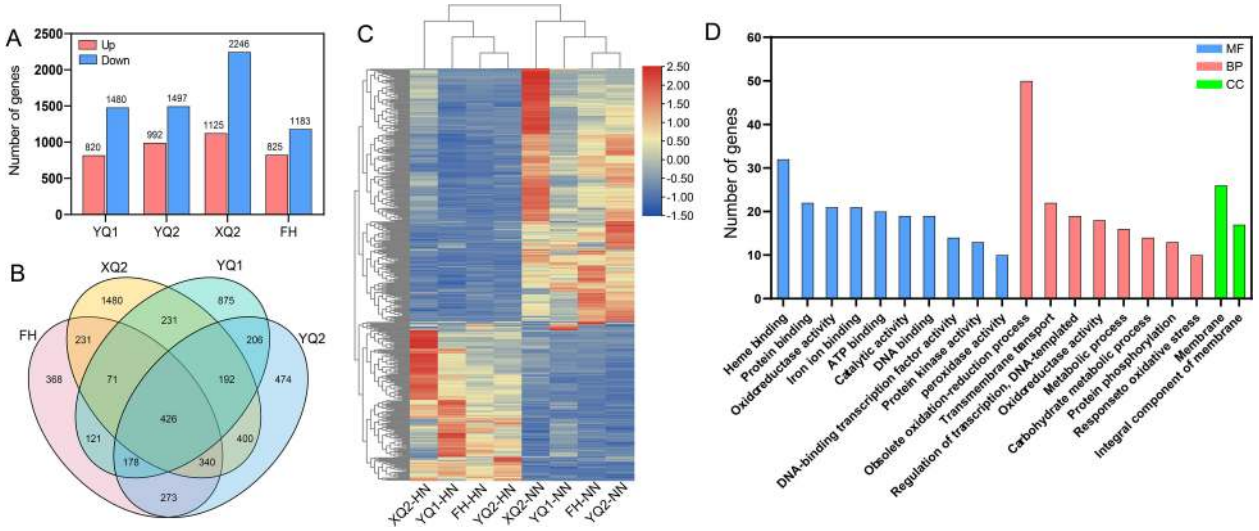

FIGURE 4
Analysis of DEGs in different TB varieties under high NH_4^+ treatment. **(A)** The DEGs number of each variety under high NH_4^+. **(B)** Venn diagram showing the overlapping DEGs among the four comparisons. **(C)** Heatmap of 426 common DEGs. **(D)** Gene ontology enrichment analysis of the 426 common DEGs.

more enriched into plant hormone signal transduction, phenylpropanoid biosynthesis, starch and sucrose metabolism, DNA replication, endocytosis, and ribosome. 875 YQ1-specific DEGs were more enriched into plant-pathogen interaction, plant hormone signal transduction, phenylpropanoid biosynthesis, mRNA surveillance pathway and starch, and sucrose metabolism. 474 YQ1-specific DEGs were more enriched into plant hormone signal transduction, oxidative phosphorylation, plant-pathogen interaction, phenylpropanoid biosynthesis, and carotenoid biosynthesis (Figure 6).

3.6 Integrating genomic and transcriptome analysis to identify key high NH_4^+-responsive DEGs

In a previous study, FH, XQ2, YQ1, and YQ2 were analyzed by genomic re-sequencing and generating 3,220 varied genes (Qiu et al., 2023). 443 genotype-specific high NH_4^+-responsive DEGs with genome sequence variation were found, including 65 FH-specific varied DEGs, 184 XQ2-specific varied DEGs, 132 YQ1-specific varied DEGs, and 62 YQ2-specific varied DEGs (Figure 7A). GO enrichment analysis showed that the 443 genotype-specific varied DEGs were more enriched into integral component of membrane, membrane, ATP binding, protein binding, DNA binding, protein kinase activity, heme binding, obsolete oxidation-reduction process, protein phosphorylation, metabolic process, transmembrane transport, and regulation of transcription DNA-templated (Figure 7B).

The key **h**igh NH_4^+-responsive varied DEGs involved in several pathways were analyzed (Figure 7C). In FH, three receptor-like protein kinases (*RLK*), one TF, one hormone signaling, and one *PER* genes were found. Four *RLK* (such as *BAM1/3*), five *TF* (such as *MYB4/25*), one hormone signaling, and one *PER* genes were found in XQ2. In YQ1, ten *RLK* (such as *LECRK3/5/42* and *CRK7/10/11*), one TF (such as *MYB44/C1*), two hormone signaling, one *PER*, and two N transport and assimilation-related gene were found. In addition, two RLK, seven TF (such as *LBD29* and *RAP2-1*), one hormone signaling, and N transport and assimilation-related genes were found in YQ2 (Figure 7C). Above data provide the first-hand data for revealing the mechanism of TB root respond to high NH_4^+.

4 Discussion

4.1 High NH_4^+ inhibits root growth by affecting the antioxidant enzyme system

N is one of the key limiting factors for plant growth and crop yield (Teng et al., 2022). Previous studies have shown that an appropriate amount of N fertilizer can significantly promote plant growth, flowering, fruiting, and yield, but high NH_4^+ can inhibit plant growth (Hikosaka, 2004; Wang et al., 2022a). Improving the knowledge on physiological and molecular mechanisms of plants respond to high NH_4^+ will contribute to the improvement of the crops with high NH_4^+ tolerance and high N use efficiency. In this study, it is found that high NH_4^+ affected TB growth by hydroponic experiment, and the growth of TB root was severely limited (Figure 1). It is speculated that high NH_4^+ significantly affects the growth of roots and causes its toxicity, which in turn affects shoots growth (Liu et al., 2023b). In order to investigate the effect of high NH_4^+ on TB root, the physiological and gene expression changes involved in antioxidant enzyme system were analyzed by

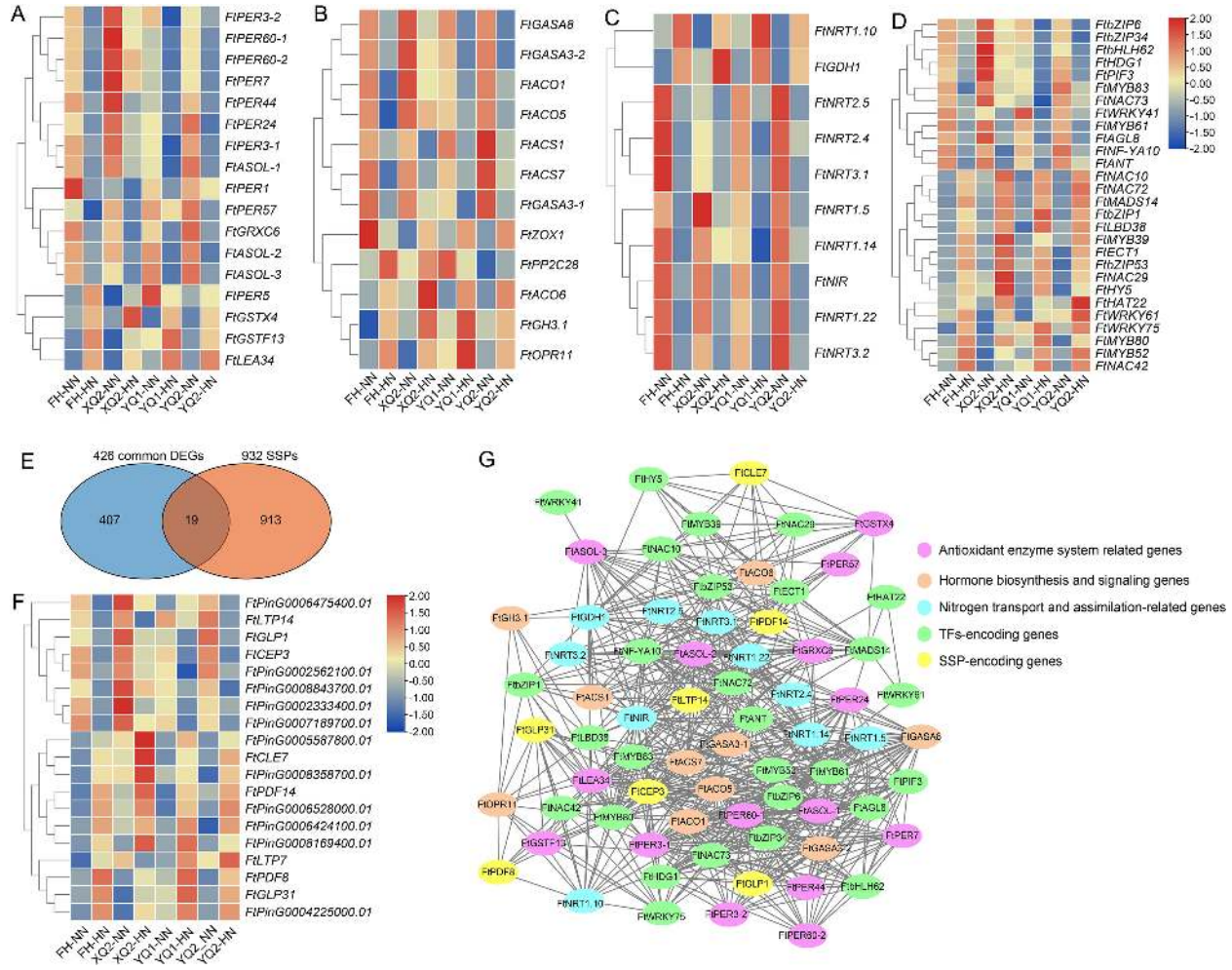

FIGURE 5
Identification of the key high NH_4^+-responsive genes from the 426 high NH_4^+-responsive DEGs. **(A-D)** Expression analysis of the genes involved in antioxidant enzyme system, hormone signaling and nitrogen transport, as well as transcription factors encoding genes. **(E)** Venn diagram showing the overlapping genes between 426 high NH_4^+-responsive DEGs and 932 *SSP* genes. **(F)** Expression analysis of the 19 DEGs encoding SSPs. Color scale on the heatmaps indicates the degree of expression: red, high expression; green, low expression. **(G)** The correlations among the key high NH_4^+-responsive DEGs. The pearson's correlation coefficient was applied for correlation analysis. The correlation index >0.8 or < – 0.8 was set as the cut-off. The results were performed by Cytoscape software.

biochemical and transcriptome analyses. High NH_4^+ significantly increased the MDA content of TB plants and affected the activities of CAT, POD, APX, and SOD (Figure 2). In tomato (*Solanum lycopersicum* L.), the activities of antioxidant enzymes including SOD, POD, and CAT were also affected significantly by high NH_4^+ (Zhang et al., 2022). Most of the genes encoding POD and APX were down-regulated by high NH_4^+ (Figure 5A). The above analysis indicated that high NH_4^+ inhibits root growth by affecting the antioxidant enzyme system, thereby suppressing plant growth. Previous studies showed that graphene oxide nanomaterials and cadmium stress enhanced CAT activity while decreased POD activity in TB roots, which is completely opposite to the results of this study (Liu et al., 2022; Ye et al., 2022). Under drought stress, SOD, CAT, and POD activities in the root of TB and its close relative species, common buckwheat (*Fagopyrum esculentum* Moench) and *Fagopyrum leptopodum*, were up-regulated (Wang et al., 2023a, 2025; Zhu et al., 2022a). Aluminum toxicity enhanced CAT activity but did not affect SOD activity in common buckwheat roots (Salazar-Chavarría et al., 2020). However, NaCl stress suppressed the activities of CAT, POD, and APX in TB roots (Yao et al., 2022). The above analysis indicates that TB roots showed diverse and complex responses to different abiotic stresses at biochemical level, the underlying mechanism is worth to be explored deeply in future study.

4.2 426 common DEGs suggest the mechanism on *Fagopyrum* genus respond to high NH_4^+

In recent years, many works for studying the mechanisms of TB in response to N were conducted, and TB was a potential model to research N response in plants (Liu et al., 2021a, 2021b, 2023a; Qiu et al., 2023). However, the mechanism on TB responds high NH_4^+

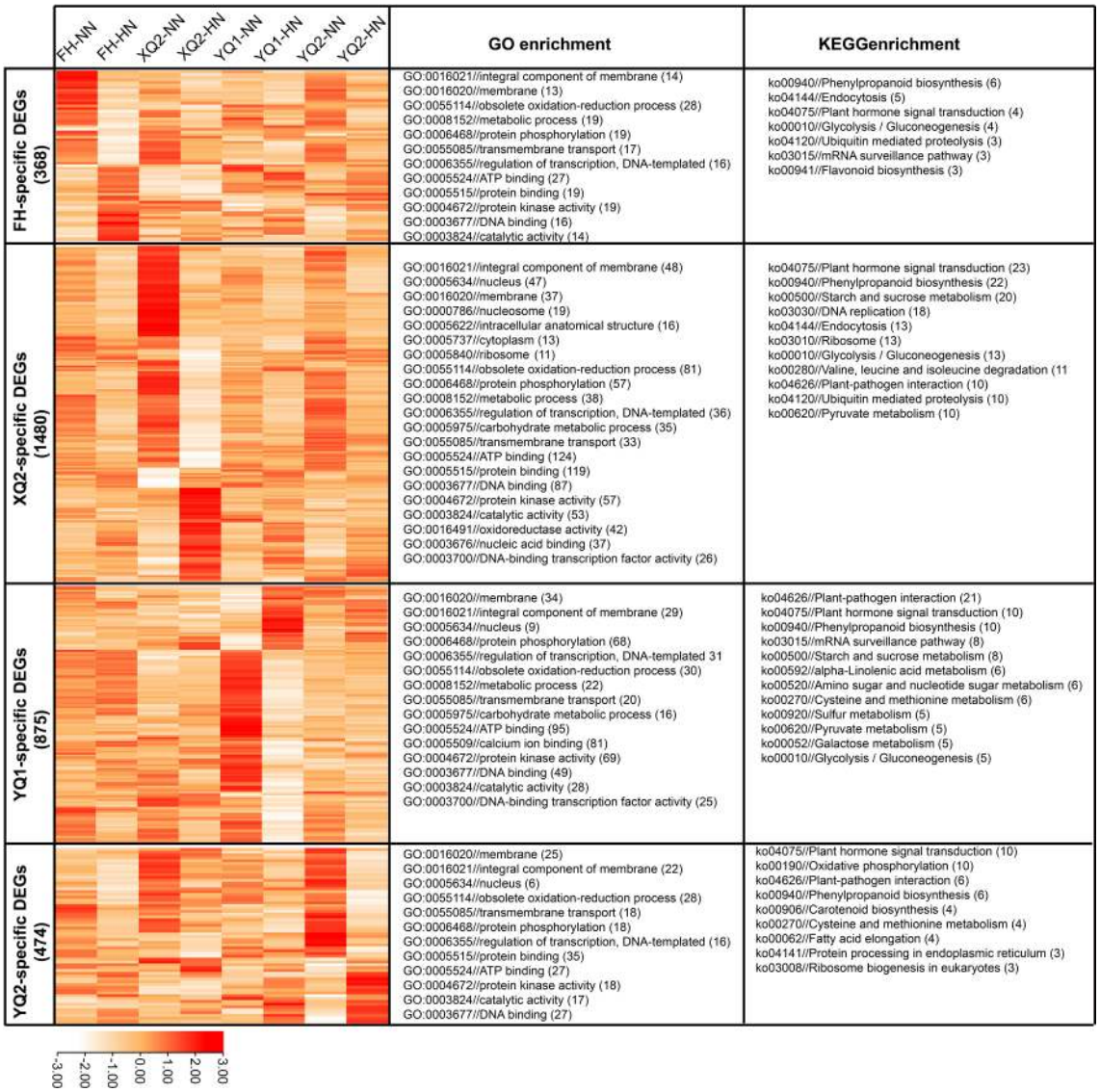

FIGURE 6
Expression analysis and GO/KEGG enrichment of the genotype-specific high NH_4^+-responsive DEGs. Color scale in the heatmaps indicates the degree of expression: red, high expression; white, low expression.

stress remains unclear. In this study, 426 common high NH_4^+-responsive DEGs were found in all four TB varieties (Figure 4B). It is found that the expression of genes involved in N uptake and utilization was significantly inhibited by high NH_4^+ (Figure 5C; Supplementary Table 5). These results are similar to the data that was reported in a previous study (Sun et al., 2021b). It is indicated that high NH_4^+ affects nutrient uptake by inhibiting the expression of nutrient uptake and utilization genes. Here, a key N transport gene, *FtNRT1.14*, showed decreased expression under high NH_4^+ condition (Figure 5C). Previous studies showed that *NRT1.1* reduced ammonium tolerance of *Arabidopsis*, and mutation of *NRT1.1* enhanced high NH_4^+ resistance (Xiao et al., 2022). The down-regulation of *FtNRT1.14* expression may help TB to survive from high NH_4^+. In addition, the expression of *FtGDH1* encoding glutamate dehydrogenase was significantly inhibited by high NH_4^+ (Figure 5C). In rice, overexpression of a fungal *GDH* gene improved tolerance to ammonium toxicity by increasing assimilation of excess NH_4^+ (Yan et al., 2021), which indicated that manipulating the ammonium assimilation may be a promising strategy for improving high NH_4^+ tolerance of crops.

Previous studies suggested that hormones regulated ammonium response in plants (Li et al., 2014, 2019; Sun et al., 2020; Pandey et al., 2024). In this study, the ETH biosynthetic genes, *FtACO1/5* and *FtACS1/7*, showed decreased expression under high NH_4^+ treatment (Figure 5B). Thus, ETH accumulation and its signaling in root may be suppressed by high NH_4^+. Previous studies showed that high NH_4^+ enhanced ethylene biosynthesis in shoots by up-regulating *ACO* and *ACS* genes, and then leading to oxidative stress under NH_4^+ stress (Li et al., 2014, 2019). Meanwhile, mutation of ETH signaling components such as ETR1 and EIN3 show greater

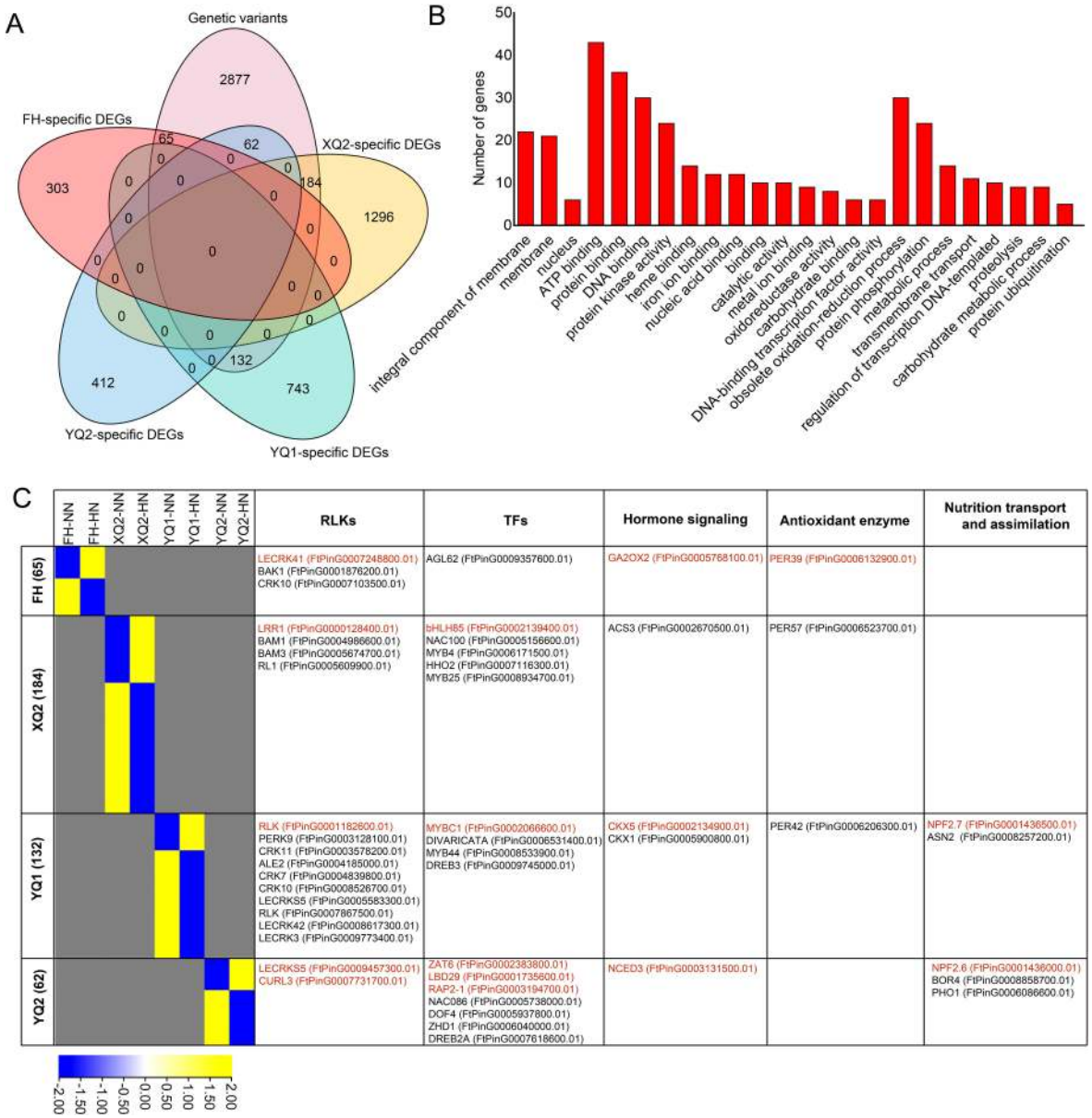

FIGURE 7
Identification of the key genotype-specific high NH_4^+-responsive DEGs with sequence variation. **(A)** Venn diagram showing the genotype-specific varied DEGs. **(B)** GO enrichment analysis of the 443 genotype-specific varied DEGs. **(C)** Heatmap analysis of the 443 genotype-specific varied DEGs. Color scale in the heatmaps indicates the degree of expression: yellow, high expression; blue, low expression. The genes marked red fond represent the up-regulated genes under high NH_4^+. The genes marked black fond represent the down-regulated genes under high NH_4^+.

NH_4^+ tolerance of *Arabidopsis*, while mutation of these negative regulators of ethylene biosynthesis improved sensitivity to high NH_4^+ (Li et al., 2013, 2014). Above analysis indicated that ETH showed different response in root and shoot, and the suppression of ETH signaling in root may be better for TB to adapt to high NH_4^+ environment.

SSP is a kind of mature polypeptide with special functions formed by proteasome cleavage, and its length is usually 5~20 amino acids (Boschiero et al., 2020). In recent years, many studies have shown that plant SSPs play an important role in N uptake and utilization. CEP and CLE peptides are main SSPs involved in the regulation of N signal transduction. CEP and CLE promote N uptake and utilization in *Arabidopsis*, soybean (*Glycine max* L.), *Lotus japonicus*, and alfalfa (*Medicago truncatula*) (Laffont et al., 2020; Lim et al., 2011; Okamoto et al., 2013, 2016). In this study, a *CLE* gene, *FtCLE7*, and a *CEP* gene, *FtCEP3*, were found in the 426 high NH_4^+-responsive genes (Figure 5F). The expression of *FtCLE7* was improved by high NH_4^+, while *FtCEP3* expression was inhibited (Figure 5F). These two genes showed higher correlations with genes involved in antioxidant enzyme system, hormone signaling, and transcriptional regulation (Figure 5G). These data indicated that *FtCLE7* and *FtCEP3* may be the core genes in high NH_4^+ response. In a previous study in alfalfa, MtCLE13 and MtCEP7 played antagonistic roles in rhizobial infection,

nodulation, and N signaling (Laffont et al., 2020). It is suggested that the up-regulation of *FtCLE7* expression and down-regulation of *FtCEP3* expression may represent a finely tuned balancing mechanism, aiming to optimize root perception and response to N in a high NH_4^+ environment. However, more studies are needed to clarify this hypothesis.

In previous studies, the functions of many TFs in regulating various abiotic and biotic stresses have been widely studied in TB. Previous studies showed found that FtNAC31 enhances salt and drought tolerance in transgenic *Arabidopsis* by increasing antioxidant enzyme activities and stress-associated genes' expression, and FtNAC10 enhanced root elongation under saline and drought stress through ABA-signaling pathway (Li et al., 2023; Zhao et al., 2022). *FtNAC10/29/42/72* genes, especially the hub gene *FtNAC72*, were found to be up-regulated by high NH_4^+ (Figures 5D, G), which may be the broad-spectrum resistance gene against abiotic stresses in TB. Some MYB in TB such as FtMYB9/13/30 regulated salt/drought tolerance by regulating different stress-responsive signaling pathways, and FtMYB12 improves cold tolerance (Gao et al., 2017; Wang et al., 2022b; Huang et al., 2018; Zhou et al., 2015). FeR2R3-MYB in common buckwheat positively regulates anthocyanin biosynthesis and drought tolerance (Luo et al., 2024). In this study, many high NH_4^+-responsive *MYB* genes including *FtMYB38/52/80* were found, these genes may mediate the crosstalk among different abiotic stresses (Figure 5D). In addition, three WRKY encoding genes, *FtWRKY41/61/75*, were found to be regulated by high NH_4^+ (Figure 5D). It is known that the WRKY widely regulating plant immunity and pathogen response. It was found that FtWRKY29 improved the tolerance to low phosphorus stress in TB, and FtWRKY46 improves salt tolerance by regulating the expression of stress-related gene (Lv et al., 2020; Wang et al., 2023b). Therefore, WRKY TFs may be the important regulatory factors for improving the tolerance and adaptation of TB to varied stress environments.

4.3 Transcriptome and genomic analysis revealed the potential genes for improving the tolerance of TB to high NH_4^+

In this study, 443 genotype-specific high NH_4^+-responsive DEGs with genome sequence variation were found (Figure 7). FH showed less sensitive to HN stress than other three varieties (Supplementary Figure 3), these NH_4^+-responsive genes including *FtPER39*, *FtGA2OX2*, and *FtAGL62* may help FH to cope with high NH_4^+ stress (Figure 7C). *FtPER39* (FtPinG0002970300.01) encodes peroxidase, which can hydrolyze hydrogen peroxide and protect plants from stress. The expression of *FtGA2OX2* (FtPinG0000400800.01) encoding gibberellin 2-beta-dioxygenase, the key enzyme in GA signaling, was up-regulated by high NH_4^+. *OsGA2ox8* in rice improved the tolerance of plants to osmotic stress (Wang et al., 2021), and *Arabidopsis AtGA2ox9* contributes to freezing tolerance (Lange et al., 2020). In a recent study, *Arabidopsis GA2OX6* and *GA2OX8* regulated root cell elongation by mediating IAA-GA cross talk (Kubalová et al., 2025). Thus, it is indicated that the up-regulation of *FtGA2OX2* may contribute to high NH_4^+ tolerance by regulating root growth. The *MADS* gene *FtAGL62* showed significant response to high NH_4^+ in FH. A *MADS* gene in barley, *HvMADS27*, regulates root architecture in response to high NH_4^+ (Smoczynska et al., 2022). Meanwhile, many other TFs were found from the 443 genotype-specific DEGs in other three varieties, such as *MYB* and *LBD* genes (Figure 7C). In a previous study suggested *MYB28* and *MYB29* improved the tolerance of *Arabidopsis* to high NH_4^+ (Coleto et al., 2021). High NH_4^+ treatment significantly induced the expression of *FtLBD29* in TB (Figure 7C). In rice, OsLBD37/38/39 collaboratively alleviate excessive N stress by inhibit the expression of *OsNRT2.1/2.2/2.3* (Zhu et al., 2022b). These TFs provided candidate genes for investigating the transcriptional regulation mechanism of TB respond to high NH_4^+.

There are 19 genes encoding RLK were found in the 443 genotype-specific DEGs, and most of these genes were inhibited by high NH_4^+ (Figure 7C). Two *RLK* genes, BAM1 (FtPinG0004986600.01) and BAM3 (FtPinG0005674700.01) encoding BARELY ANY MERISTEM. In *Arabidopsis*, BAM1/2/3 were identified as the receptor of CLE peptide mediated signaling, and the participating in regulating root meristem tissue patterning and protophloem differentiation driven by CLE (Hu et al., 2022; Zhang et al., 2024). In this study, a *CLE* gene, *FtCLE7*, showed response to high NH_4^+ (Figure 5F), which indicated that it may be worthy to research the function of FtCLE7-BAM1/3 signaling in high NH_4^+ response. In addition, SSP acts as a signal molecule to exchange information between cells and cells by interacting with RLKs on the cell membrane, thereby activating downstream genes or initiating related signal transduction processes (Matsubayashi, 2014). Thus, these genotype-specific varied *RLK* genes provide the candidates for identifying the receptor of SSP in high NH_4^+ response.

4.4 The proposed working model for TB in response to high NH_4^+ was suggested

Based on the above analysis, the working model for TB in response to high NH_4^+ is summarized in Figure 8. High NH_4^+ stress is initially perceived by RLKs, SSP, and hormone-mediated signaling in root cells, and then transmitting signals to TFs. These TFs then regulate the expression of downstream genes. This might involve inhibiting most N transport and assimilation genes to mitigate toxicity, and modulating the antioxidant enzyme system to scavenge reactive oxygen species. In this model, the key SSP, FtCLE7 and FtCEP3 may pass the stress signals to their receptors belonging to RLKs on cell membrane. Meanwhile, down-regulation of ETH biosynthesis and signaling may help TB to adapt to high NH_4^+ environment by maintaining root growth.

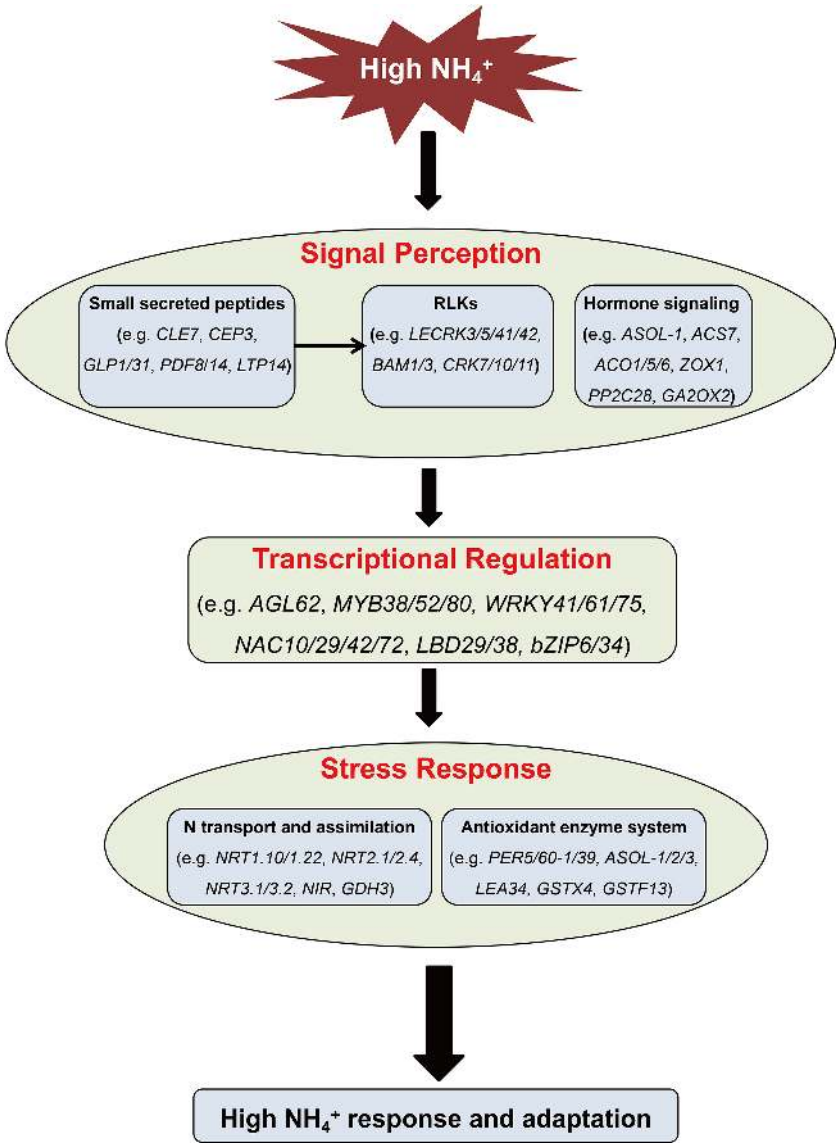

FIGURE 8
The proposed working model for TB in response to high ammonium stress.

5 Conclusion

In conclusion, the morphological and transcriptome changes of roots in TB under high NH_4^+ conditions were analyzed for the first time. High NH_4^+ reduced TB growth through hydroponic experiment. High NH_4^+ inhibits root growth and causes its toxicity, which in turn affects shoots growth. Biochemical analysis showed that high NH_4^+ resulted in the changes in the activities of antioxidant enzymes in roots. The roots of the TB seedlings under high NH_4^+ conditions were selected for transcriptome analysis. In total 426 High NH_4^+-responsive DEGs were identified. Most of the DEGs involved in antioxidant enzyme system, hormone biosynthesis and signaling, and N transport and assimilation were down-regulated by high NH_4^+. Suppression of ETH signaling in root may be better for TB to adapt to high NH_4^+ environment. 19 SSPs encoding genes were found to be involved in high NH_4^+ response, including *FtCLE7* and *FtCEP3*. The up-regulation of *FtCLE7* expression and down-regulation of *FtCEP3* expression may help plants to optimize root perception and response to high NH_4^+. The core genes in regulating high NH_4^+ response of TB were identified by co-expression analysis, such as *FtNRT1.14*, *FtMYB61/52*, *FtbZIP6/34*, *FtNAC72/73*, *FtLTP14*, and *FtCEP3*. Additionally, 443 genotype-specific high NH_4^+-responsive DEGs with sequence variation were identified by integrating transcriptome and whole-genome re-sequencing analysis, including 17 *TFs* such as *MYB*, *MADS*, and *LBD* and 19 *RLKs* such as *FtBAM1/3*. This study will provide new insight into molecular response to high NH_4^+, and provides candidate genes for improving N use efficiency and high NH_4^+ tolerance of crops through genetic manipulation.

Data availability statement

The datasets presented in this study can be found in online repositories. The names of the repository/repositories and accession number(s) can be found in the article/supplementary material.

Author contributions

CL: Funding acquisition, Methodology, Supervision, Writing – original draft, Writing – review & editing, Project administration. JW: Data curation, Investigation, Writing – original draft. QQ: Investigation, Methodology, Writing – original draft. DYX: Investigation, Writing – original draft. XW: Data curation, Writing – original draft. JY: Investigation, Writing – original draft. XZ: Formal Analysis, Writing – review & editing. MT: Investigation, Writing – original draft. YW: Supervision, Writing – review & editing. WS: Data curation, Writing – original draft. DX: Funding acquisition, Investigation, Writing – review & editing.

Funding

The author(s) declare financial support was received for the research and/or publication of this article. This research was supported by National Natural Sciences Foundation of China (No. 32301850) and China Agriculture Research System (No. CARS-07-B-1).

Conflict of interest

The authors declare that the research was conducted in the absence of any commercial or financial relationships that could be construed as a potential conflict of interest.

Generative AI statement

The author(s) declare that no Generative AI was used in the creation of this manuscript.

Any alternative text (alt text) provided alongside figures in this article has been generated by Frontiers with the support of artificial intelligence and reasonable efforts have been made to ensure accuracy, including review by the authors wherever possible. If you identify any issues, please contact us.

Publisher's note

All claims expressed in this article are solely those of the authors and do not necessarily represent those of their affiliated organizations, or those of the publisher, the editors and the reviewers. Any product that may be evaluated in this article, or claim that may be made by its manufacturer, is not guaranteed or endorsed by the publisher.

Supplementary material

The Supplementary Material for this article can be found online at: https://www.frontiersin.org/articles/10.3389/fpls.2025.1669365/full#supplementary-material.

SUPPLEMENTARY FIGURE 1
Architectural changes of seedlings as affected by high NH_4^+.

SUPPLEMENTARY FIGURE 2
Validation of expression profile through qRT-PCR. A total of 12 genes were validated using qRT-PCR against their expression profile from RNA-seq. The relative expression levels of gene were quantitated using $2^{-\Delta\Delta Ct}$.

SUPPLEMENTARY FIGURE 3
Cluster analysis of four TB varieties based the fold changes of root weight, total root length, primary root length, root surface area and root volume under 1 and 100 mmol/L NH_4^+.

References

Bittsánszky, A., Pilinszky, K., Gyulai, G., and Komives, T. (2015). Overcoming ammonium toxicity. *Plant Sci.* 231, 184–190. doi: 10.1016/j.plantsci.2014.12.005

Boschiero, C., Dai, X., Lundquist, P. K., Roy, S., Christian de Bang, T., Zhang, S., et al. (2020). MtSSPdb: The *Medicago truncatula* small secreted peptide database. *Plant Physiol.* 183, 399–413. doi: 10.1104/pp.19.01088

Coleto, I., Bejarano, I., Marín-Peña, A. J., Medina, J., Rioja, C., Burow, M., et al. (2021). *Arabidopsis thaliana* transcription factors MYB28 and MYB29 shape ammonium stress responses by regulating Fe homeostasis. *New Phytol.* 229, 1021–1035. doi: 10.1111/nph.16918

Di, D. W., Sun, L., Wang, M., Wu, J., Kronzucker, H. J., Fang, S., et al. (2021). WRKY46 promotes ammonium tolerance in *Arabidopsis* by repressing NUDX9 and indole-3-acetic acid-conjugating genes and by inhibiting ammonium efflux in the root elongation zone. *New Phytol.* 232, 190–207. doi: 10.1111/nph.17554

Esteban, R., Ariz, I., Cruz, C., and Moran, J. F. (2016). Review: mechanisms of ammonium toxicity and the quest for tolerance. *Plant Sci.* 248, 92–101. doi: 10.1016/j.plantsci.2016.04.008

Gao, F., Zhou, J., Deng, R. Y., Zhao, H. X., Li, C. L., Chen, H., et al. (2017). Overexpression of a tartary buckwheat R2R3-MYB transcription factor gene, *FtMYB9*, enhances tolerance to drought and salt stresses in transgenic *Arabidopsis*. *J. Plant Physiol.* 214, 81–90. doi: 10.1016/j.jplph.2017.04.007

Hikosaka, K. (2004). Interspecific difference in the photosynthesis-nitrogen relationship: patterns, physiological causes, and ecological importance. *J. Plant Res.* 117, 481–494. doi: 10.1007/s10265-004-0174-2

Hu, C., Zhu, Y., Cui, Y., Zeng, L., Li, S., Meng, F., et al. (2022). A CLE-BAM-CIK signalling module controls root protophloem differentiation in *Arabidopsis*. *New Phytol.* 233, 282–296. doi: 10.1111/nph.17791

Huang, Y., Zhao, H., Gao, F., Yao, P., Deng, R., Li, C., et al. (2018). A R2R3-MYB transcription factor gene, *FtMYB13*, from Tartary buckwheat improves salt/drought tolerance in *Arabidopsis*. *Plant Physiol. Biochem.* 132, 238–248. doi: 10.1016/j.plaphy.2018.09.012

Konishi, N., and Ma, J. F. (2021). Three polarly localized ammonium transporter 1 members are cooperatively responsible for ammonium uptake in rice under low ammonium condition. *New Phytol.* 232, 1778–1792. doi: 10.1111/nph.17679

Kubalová, M., Griffiths, J., Müller, K., Levenets, L., Tylová, E., Tarkowská, D., et al. (2025). Gibberellin-deactivating GA2OX enzymes act as a hub for auxin-gibberellin cross talk in *Arabidopsis thaliana* root growth regulation. *Proc. Natl. Acad. Sci. U S A.* 122, e2425574122. doi: 10.1073/pnas.2425574122

Laffont, C., Ivanovici, A., Gautrat, P., Brault, M., Djordjevic, M. A., and Frugier, F. (2020). The NIN transcription factor coordinates CEP and CLE signaling peptides that regulate nodulation antagonistically. *Nat. Commun.* 11, 3167. doi: 10.1038/s41467-020-16968-1

Lange, T., Krämer, C., and Pimenta Lange, M. J. (2020). The class III gibberellin 2-oxidases AtGA2ox9 and AtGA2ox10 contribute to cold stress tolerance and fertility. *Plant Physiol.* 184, 478–486. doi: 10.1104/pp.20.00594

Leng, X., Wang, H., Cao, L., Chang, R., Zhang, S., Xu, C., et al. (2024). Overexpressing GLUTAMINE SYNTHETASE 1;2 maintains carbon and nitrogen balance under high-ammonium conditions and results in increased tolerance to ammonium toxicity in hybrid poplar. *J. Exp. Bot.* 75, 4052–4073. doi: 10.1093/jxb/erae124

Li, G., Li, B., Dong, G., Feng, X., Kronzucker, H. J., and Shi, W. (2013). Ammonium-induced shoot ethylene production is associated with the inhibition of lateral root formation in *Arabidopsis*. *J. Exp. Bot.* 64, 1413–1425. doi: 10.1093/jxb/ert019

Li, J., Li, X., Jia, C., and Liu, D. (2023). Gene cloning and characterization of transcription factor *FtNAC10* in Tartary buckwheat (*Fagopyrum tataricum* (L.) Gaertn.). *Int. J. Mol. Sci.* 24, 16317. doi: 10.3390/ijms242216317

Li, B., Li, G., Kronzucker, H. J., Baluská, F., and Shi, W. (2014). Ammonium stress in *Arabidopsis*: signaling, genetic loci, and physiological targets. *Trends Plant Sci.* 19, 107–114. doi: 10.1016/j.tplants.2013.09.004

Li, H., Lv, Q., Shi, T., Jian, Y., Ran, B., Cheng, Y., et al. (2025). The complete reference genome of Tartary buckwheat and its mutation library provide important resources for genetic studies and breeding. *Cell Rep.* 44, 115621. doi: 10.1016/j.celrep.2025.115621

Li, S., Yan, L., Zhang, W., Yi, C., Haider, S., Wang, C., et al. (2024). Nitrate alleviates ammonium toxicity in *Brassica napus* by coordinating rhizosphere and cell pH and ammonium assimilation. *Plant J.* 117, 786–804. doi: 10.1111/tpj.16529

Li, G., Zhang, L., Wang, M., Di, D., Kronzucker, H. J., and Shi, W. (2019). The *Arabidopsis AMOT1/EIN3* gene plays an important role in the amelioration of ammonium toxicity. *J. Exp. Bot.* 70, 1375–1388. doi: 10.1093/jxb/ery457

Lim, C. W., Lee, Y. W., and Hwang, C. H. (2011). Soybean nodule-enhanced CLE peptides in roots act as signals in GmNARK-mediated nodulation suppression. *Plant Cell Physiol.* 52, 1613–1627. doi: 10.1093/pcp/pcr091

Liu, K., Chen, Y., Li, S., Wang, W., Zhang, W., Zhang, H., et al. (2023b). Differing responses of root morphology and physiology to nitrogen application rates and their relationships with grain yield in rice. *Crop J.* 11, 618–627. doi: 10.1016/j.cj.2022.07.019

Liu, C., Qiu, Q., Zou, B., Wu, Q., Ye, X., Wan, Y., et al. (2023a). Comparative transcriptome and genome analysis unravels the response of Tatary buckwheat root to nitrogen deficiency. *Plant Physiol. Biochem.* 196, 647–660. doi: 10.1016/j.plaphy.2023.02.023

Liu, C., Sun, L., Sun, Y., You, X., Wan, Y., Wu, X., et al. (2022). Integrating transcriptome and physiological analyses to elucidate the molecular responses of buckwheat to graphene oxide. *J. Hazard. Mater.* 424, 127443. doi: 10.1016/j.jhazmat.2021.127443

Liu, Y., and von Wirén, N. (2017). Ammonium as a signal for physiological and morphological responses in plants. *J. Exp. Bot.* 68, 2581–2592. doi: 10.1093/jxb/erx086

Liu, C., Wu, Q., Sun, L., You, X., Ye, X., Wan, Y., et al. (2021a). Nitrate dose-responsive transcriptome analysis identifies transcription factors and small secreted peptides involved in nitrogen response in Tartary buckwheat. *Plant Physiol. Biochem.* 162, 1–13. doi: 10.1016/j.plaphy.2021.02.027

Liu, C., Xiang, D., Wu, Q., Ye, X., Yan, H., Zhao, G., et al. (2021b). Dynamic transcriptome and co-expression analysis suggest the potential roles of small secreted peptides from Tartary buckwheat (*Fagopyrum tataricum*) in low nitrogen stress response. *Plant Sci.* 313, 111091. doi: 10.1016/j.plantsci.2021.111091

Luo, Y., Xu, X., Yang, L., Zhu, X., Du, Y., and Fang, Z. (2024). A R2R3-MYB transcription factor, FeR2R3-MYB, positively regulates anthocyanin biosynthesis and drought tolerance in common buckwheat (*Fagopyrum esculentum*). *Plant Physiol. Biochem.* 217, 109254. doi: 10.1016/j.plaphy.2024.109254

Lv, B., Wu, Q., Wang, A., Li, Q., Dong, Q., Yang, J., et al. (2020). A WRKY transcription factor, FtWRKY46, from Tartary buckwheat improves salt tolerance in transgenic *Arabidopsis thaliana*. *Plant Physiol. Biochem.* 147, 43–53. doi: 10.1016/j.plaphy.2019.12.004

Matsubayashi, Y. (2014). Posttranslationally modified small-peptide signals in plants. *Annu. Rev. Plant Biol.* 65, 385–413. doi: 10.1146/annurev-arplant-050312-120122

Okamoto, S., Shinohara, H., Mori, T., Matsubayashi, Y., and Kawaguchi, M. (2013). Root-derived CLE glycopeptides control nodulation by direct binding to HAR1 receptor kinase. *Nat. Commun.* 4, 2191. doi: 10.1038/ncomms3191

Okamoto, S., Tabata, R., and Matsubayashi, Y. (2016). Long-distance peptide signaling essential for nutrient homeostasis in plants. *Curr. Opin. Plant Biol.* 34, 35–40. doi: 10.1016/j.pbi.2016.07.009

Pandey, A., Devi, L. L., Gupta, S., Prasad, P., Agrwal, K., Asif, M. H., et al. (2024). Jasmonate signaling modulates root growth by suppressing iron accumulation during ammonium stress. *Plant Physiol.* 196, 2213–2231. doi: 10.1093/plphys/kiae390

Qiu, Q., Xiang, D., Li, Q., Wang, H., Wan, Y., Wu, Q., et al. (2023). Interkingdom multi-omics analysis reveals the effects of nitrogen application on growth and rhizosphere microbial community of Tartary buckwheat. *Front. Microbiol.* 14. doi: 10.3389/fmicb.2023.1240029

Salazar-Chavarría, V., Sánchez-Nieto, S., and Cruz-Ortega, R. (2020). Fagopyrum esculentum at early stages copes with aluminum toxicity by increasing ABA levels and antioxidant system. *Plant Physiol. Biochem.* 152, 170–176. doi: 10.1016/j.plaphy.2020.04.024

Smoczynska, A., Pacak, A., Grabowska, A., Bielewicz, D., Zadworny, M., Singh, K., et al. (2022). Excess nitrogen responsive HvMADS27 transcription factor controls barley root architecture by regulating abscisic acid level. *Front. Plant Sci.* 13. doi: 10.3389/fpls.2022.950796

Sonoda, Y., Ikeda, A., Saiki, S., von Wirén, N., Yamaya, T., and Yamaguchi, J. (2003). Distinct expression and function of three ammonium transporter genes (*OsAMT1;1–1;3*) in rice. *Plant Cell Physiol.* 7, 726–734. doi: 10.1093/pcp/pcg083

Sun, L., Di, D. W., Li, G., Kronzucker, H. J., Wu, X., and Shi, W. (2020). Endogenous ABA alleviates rice ammonium toxicity by reducing ROS and free ammonium via regulation of the SAPK9-bZIP20 pathway. *J. Exp. Bot.* 71, 4562–4577. doi: 10.1093/jxb/eraa076

Sun, D., Fang, X., Xiao, C., Ma, Z., Huang, X., Su, J., et al. (2021a). Kinase SnRK1.1 regulates nitrate channel SLAH3 engaged in nitrate-dependent alleviation of ammonium toxicity. *Plant Physiol.* 186, 731–749. doi: 10.1093/plphys/kiab057

Sun, T., Wang, T., Qiang, Y., Zhao, G., Yang, J., Zhong, H., et al. (2022). CBL-interacting protein kinase OsCIPK18 regulates the Response of ammonium toxicity in rice roots. *Front. Plant Sci.* 13. doi: 10.3389/fpls.2022.863283

Sun, T., Zhang, J., Zhang, Q., Li, X., Li, M., Yang, Y., et al. (2021b). Integrative physiological, transcriptome, and metabolome analysis reveals the effects of nitrogen sufficiency and deficiency conditions in apple leaves and roots. *Environ. Exp. Bot.* 192, 104633. doi: 10.1016/j.envexpbot.2021.104633

Teng, R.-M., Yang, N., Liu, C.-F., Chen, Y., Wang, Y., and Zhuang, J. (2022). CsLBD37, a LBD/ASL transcription factor, affects nitrate response and flowering of tea plant. *Sci. Hortic.* 306, 111457. doi: 10.1016/j.scienta.2022.111457

Wang, S., Cao, X., Li, H., Shan, Z., Wang, T., Li, C., et al. (2025). FtbHLH1, a transcription factor that interacts with FtATG8a, enhances the drought stress response in Tartary buckwheat. *Plant Physiol. Biochem.* 222, 109729. doi: 10.1016/j.plaphy.2025.109729

Wang, Y., Du, F., Wang, J., Li, Y., Zhang, Y., Zhao, X., et al. (2021). Molecular dissection of the gene *OsGA2ox8* conferring osmotic stress tolerance in rice. *Int. J. Mol. Sci.* 22, 9107. doi: 10.3390/ijms22179107

Wang, J., Hussain, S., Sun, X., Zhang, P., Javed, T., Dessoky, E. S., et al. (2022a). Effects of nitrogen application rate under straw incorporation on photosynthesis, productivity and nitrogen use efficiency in winter wheat. *Front. Plant Sci.* 13. doi: 10.3389/fpls.2022.862088

Wang, A., Liu, Y., Li, Q., Li, X., Zhang, X., Kong, J., et al. (2023a). *FlbZIP12* gene enhances drought tolerance via modulating flavonoid biosynthesis in *Fagopyrum leptopodum*. *Front. Plant Sci.* 14. doi: 10.3389/fpls.2023.1279468

Wang, S., Lv, B., Wang, A., Hu, J., Wu, Q., and Li, C. (2023b). Cloning and functional characterization of *FtWRKY29*, a low phosphorus stress-inducible transcription factor in Tartary buckwheat. *Plant Physiol. Biochem.* 203, 107997. doi: 10.1016/j.plaphy.2023.107997

Wang, S., Wu, H., Cao, X., Fan, W., Li, C., Zhao, H., et al. (2022b). Tartary buckwheat FtMYB30 transcription factor improves the salt/drought tolerance of transgenic *Arabidopsis* in an ABA-dependent manner. *Physiol. Plant* 174, e13781. doi: 10.1111/ppl.13781

Xiao, C., Sun, D., Liu, B., Fang, X., Li, P., Jiang, Y., et al. (2022). Nitrate transporter NRT1.1 and anion channel SLAH3 form a functional unit to regulate nitrate-dependent alleviation of ammonium toxicity. *J. Integr. Plant Biol.* 64, 942–957. doi: 10.1111/jipb.13239

Xu, G., Fan, X., and Miller, A. J. (2012). Plant nitrogen assimilation and use efficiency. *Annu. Rev. Plant Biol.* 63, 153–182. doi: 10.1146/annurev-arplant-042811-105532

Yan, L., Gong, Y., Luo, Q., Dai, G. X., Teng, Z., He, Y., et al. (2021). Heterologous expression of fungal *AcGDH* alleviates ammonium toxicity and suppresses photorespiration, thereby improving drought tolerance in rice. *Plant Sci.* 305, 110769. doi: 10.1016/j.plantsci.2020.110769

Yan, Y., Zhang, Z., Sun, H., Liu, X., Xie, J., Qiu, Y., et al. (2023). Nitrate confers rice adaptation to high ammonium by suppressing its uptake but promoting its assimilation. *Mol. Plant* 16, 1871–1874. doi: 10.1016/j.molp.2023.11.008

Yang, Q., Wang, G., Ma, J., Zhou, H., He, L., and Qu, C. (2025). Overexpression of *pxAlaAT3* in *Populus × xiaohei* alleviates root growth inhibition under ammonium nitrogen stress. *Plant Cell Rep.* 44, 126. doi: 10.1007/s00299-025-03516-8

Yao, X., Zhou, M., Ruan, J., Peng, Y., Ma, C., Wu, W., et al. (2022). Physiological and biochemical regulation mechanism of exogenous hydrogen peroxide in alleviating NaCl stress toxicity in Tartary buckwheat (*Fagopyrum tataricum* (L.) Gaertn). *Int. J. Mol. Sci.* 23, 10698. doi: 10.3390/ijms231810698

Ye, X., Li, Q., Liu, C., Wu, Q., Wan, Y., Wu, X., et al. (2022). Transcriptomic, cytological, and physiological analyses reveal the potential regulatory mechanism in Tartary buckwheat under cadmium stress. *Front. Plant Sci.* 13. doi: 10.3389/fpls.2022.1004802

Zhang, H., Wang, Q., Blanco-Touriñán, N., and Hardtke, C. S. (2024). Antagonistic CLE peptide pathways shape root meristem tissue patterning. *Nat. Plants* 10, 1900–1908. doi: 10.1038/s41477-024-01838-1

Zhang, L., Li, X., Ma, B., Gao, Q., Du, H., Han, Y., et al. (2017). The Tartary buckwheat genome provides insights into rutin biosynthesis and abiotic stress tolerance. *Mol. Plant* 10, 1224–1237. doi: 10.1016/j.molp.2017.08.013

Zhang, Y., Yu, S., Li, Z., Chang, T., Xu, Q., Xu, H., et al. (2022). Effects of excessive nitrogen fertilizer and soil moisture deficiency on antioxidant enzyme system and osmotic adjustment in tomato seedlings. *Int. J. Agr. Biol. Eng.* 15, 127–134. doi: 10.25165/j.ijabe.20221502.5555

Zhao, J. L., Wu, Q., Wu, H. L., Wang, A. H., Wang, X. L., Li, C. L., et al. (2022). FtNAC31, a Tartary buckwheat NAC transcription factor, enhances salt and drought tolerance in transgenic *Arabidopsis*. *Plant Physiol. Biochem.* 191, 20–33. doi: 10.1016/j.plaphy.2022.09.016

Zheng, X., He, K., Kleist, T., Chen, F., and Luan, S. (2015). Anion channel SLAH3 functions in nitrate-dependent alleviation of ammonium toxicity in *Arabidopsis*. *Plant Cell Environ.* 38, 474–486. doi: 10.1111/pce.12389

Zhou, M., Wang, C., Qi, L., Yang, X., Sun, Z., Tang, Y., et al. (2015). Ectopic expression of *Fagopyrum tataricum FtMYB12* improves cold tolerance in *Arabidopsis thaliana*. *J. Plant Growth. Regul.* 34, 362–371. doi: 10.1007/s00344-014-9472-7

Zhu, X., Hou, Z., Xu, X., Xiong, Z., Chen, Y., Yang, L., et al. (2022a). TMT-based comparative proteomics reveals the role of acyl-CoA oxidase 4 in enhancing the drought stress tolerance in common buckwheat (*Fagopyrum esculentum*). *Int. J. Biol. Macromol.* 215, 262–271. doi: 10.1016/j.ijbiomac.2022.06.002

Zhu, X., Wang, D., Xie, L., Zhou, T., Zhao, J., Zhang, Q., et al. (2022b). Rice transcription factors OsLBD37/38/39 regulate nitrate uptake by repressing *OsNRT2.1/2.2/2.3* under high-nitrogen conditions. *Crop J.* 10, 1623–1632. doi: 10.1016/j.cj.2022.03.011